

N^1 -Substituted Thymine Derivatives as Mitochondrial Thymidine Kinase (TK-2) Inhibitors

Ana-Isabel Hernández,[#] Olga Familiar,[#] Ana Negri,[§] Fátima Rodríguez-Barrios,[§] Federico Gago,[§] Anna Karlsson,[‡] María-José Camarasa,[#] Jan Balzarini,[†] and María-Jesús Pérez-Pérez^{#*}

Instituto de Química Médica (C.S.I.C.), Juan de la Cierva 3, E-28006 Madrid, Spain, Departamento de Farmacología, Universidad de Alcalá, E-28871 Alcalá de Henares, Madrid, Spain, Karolinska Institute, S-141 86 Huddinge/Stockholm, Sweden, Rega Institute for Medical Research, Katholieke Universiteit Leuven, B-3000 Leuven, Belgium

Received September 5, 2006

Novel N^1 -substituted thymine derivatives related to 1-[(Z)-4-(triphenylmethoxy)-2-butenyl]thymine have been synthesized and evaluated against thymidine kinase-2 (TK-2) and related nucleoside kinases [i.e., *Drosophila melanogaster* deoxynucleoside kinase (*Dm*-dNK) and herpes simplex virus type 1 thymidine kinase (HSV-1 TK)]. The thymine base has been tethered to a distal triphenylmethoxy moiety through a polymethylene chain ($n = 3-8$) or through a (2-ethoxy)ethyl spacer. Moreover, substitutions at position 4 of one of the phenyl rings of the triphenylmethoxy moiety have been performed. Compounds with a hexamethylene spacer (**18**, **26b**, **31**) displayed the highest inhibitory values against TK-2 ($IC_{50} = 0.3-0.5 \mu M$). Compound **26b** competitively inhibited TK-2 with respect to thymidine and uncompetitively with respect to ATP. A rationale for the biological data was provided by docking some representative inhibitors into a homology-based model of human TK-2. Moreover, two of the most potent TK-2 inhibitors (**18** and **26b**) that also inhibit HSV-1 TK were able to reverse the cytostatic activity of 1-(β -D-arabinofuranosyl)thymine (Ara-T) and ganciclovir in HSV-1 TK-expressing OST-TK⁻/HSV-1 TK⁺ cell cultures.

Introduction

Mitochondrial (mt) thymidine kinase (TK-2) belongs to the family of mammalian deoxynucleoside kinases (dNKs) that catalyze the phosphorylation of deoxynucleosides to their corresponding deoxynucleoside monophosphates by γ -phosphoryl transfer from ATP (or other nucleoside triphosphates).^{1,2} Deoxynucleoside kinases are instrumental in the activation of deoxynucleoside analogues with biological and therapeutic properties, a large number of them being used in the treatment of viral diseases and cancer.³ Besides the activation of nucleoside analogues with pharmacological properties, dNKs have a fundamental role in the salvage pathway of deoxynucleotide synthesis. Moreover, mitochondrial DNA (mtDNA) synthesis, which occurs rather independently of nuclear DNA synthesis, is maintained during the whole cell cycle. In resting cells, TK-2 is the predominant, if not the exclusive, dThd-phosphorylating enzyme, and TK-2 is suggested to play a key role in the mitochondrial salvage pathway to provide the nucleotides for mtDNA synthesis. Interestingly, critical point mutations in the gene encoding TK-2 have been correlated to mtDNA disorders, further supporting an essential role of TK-2 in mtDNA synthesis.^{4,5}

Long-term treatment with antiviral nucleoside analogues such as zidovudine (AZT) or 2'-fluoro-5-iodo-(1- β -D-arabinofuranosyl)uracil (FIAU) has been associated with severe mitochondrial toxicity.^{6,7} Since these nucleoside analogues are phosphorylated by TK-2, it can be speculated that their corresponding triphosphates may accumulate inside the mitochondria thereby compromising mtDNA synthesis. Several nucleoside analogues have been linked to genetic mtDNA depletion syndromes and mtDNA

depletion.⁵ Still, the mechanisms by which these nucleoside analogues exert their mitochondrial toxicity are not fully understood.⁷

On the basis of its amino acid sequence, TK-2 belongs to a large group of dNKs that includes other human enzymes such as deoxycytidine kinase (dCK) and deoxyguanosine kinase (dGK), together with other dNKs of different origins, such as the multisubstrate dNK of the fruitfly, *Drosophila melanogaster* (*Dm*-dNK), and to a lesser extent, with the thymidine kinase of herpes simplex virus type 1 (HSV-1 TK).² The amino acid sequence identity between human TK-2 and *Dm*-dNK is about 40%, and there are no long insertions or deletions in their genes. In 2001, the structure of *Dm*-dNK in complex with dCyd was solved.⁸ Two other complexes of *Dm*-dNK with either dThd or dTTP also have been reported.⁹ It is interesting to note that although *Dm*-dNK shares only 10% of amino acid sequence identity with HSV-1 TK, the core structure of these two enzymes has a very similar overall fold. Given the sequence similarity between TK-2 and *Dm*-dNK, and to a lesser extent, HSV-1 TK, the testing of compounds has been performed in many cases against the three enzymes. The information gained from these experiments can also be relevant to further explore similarities and differences among these related enzymes.

From the features described above, it can be concluded that TK-2 is implicated in the phosphorylation of pyrimidine nucleosides that is required for mtDNA synthesis. TK-2 could also be involved in the mitochondrial toxicity associated with prolonged treatment with antiviral nucleoside analogues. However, there are still many open questions regarding the real contribution of TK-2 to these issues. Our research groups have been involved in the identification of TK-2 inhibitors that could become valuable tools not only to unravel the role of TK-2 in the maintenance and homeostasis of mitochondrial dNTP pools but also to help clarify the contribution of TK-2-catalyzed phosphorylation of certain antiviral drugs to their mitochondrial toxicity. Such inhibitors could also be helpful to investigate the activity of TK-1 and TK-2 in different cell types. In 2002, we

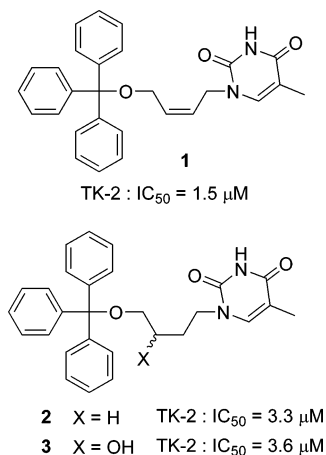
* To whom correspondence should be addressed. Phone: 34 91 5622900 ext 411. Fax: 34 91 5644853. E-mail: mjperez@iqm.csic.es.

[#] Instituto de Química Médica (C.S.I.C.).

[§] Universidad de Alcalá.

[‡] Karolinska Institute.

[†] Katholieke Universiteit Leuven.

Chart 1. Structural Formulas of Previously Described Acyclic Nucleosides TK-2 Inhibitors

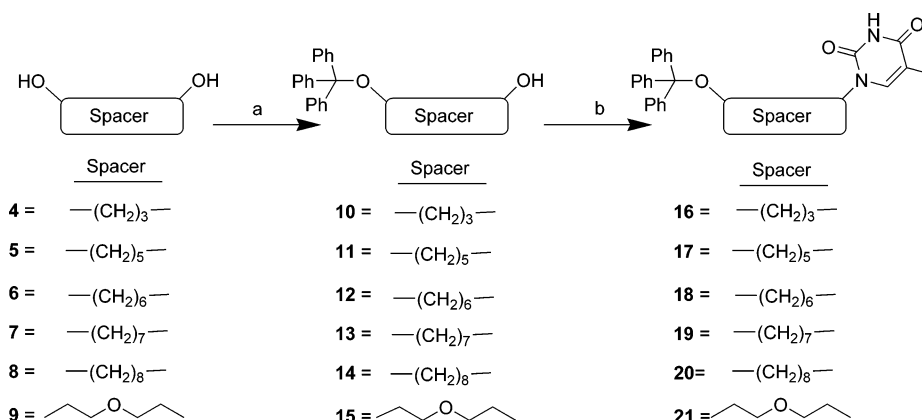
described the first acyclic nucleoside analogues that inhibited TK-2, the prototype compound being 1-[(*Z*)-4-(triphenylmethoxy)-2-butenyl]thymine (**1**) (Chart 1).¹⁰ The structure–activity relationship studies performed with a different series of analogues of the lead compound **1** have shown the following features:¹¹ (i) the nucleic base is crucial for the interaction of these inhibitors with the target enzyme(s) (e.g., it has been established that competitive inhibition by **1** is exerted with respect to thymidine,¹² suggesting that this inhibitor binds at the substrate binding site); (ii) the spacer connecting the nucleic base and the distal substituent has a major impact on the potency and selectivity of the inhibitors against TK-2 and related enzymes. Although most of the synthesized structures contain a (*Z*)-2-butenyl linker, increasing the conformational freedom of the spacer (as in compounds **2** and **3**)¹⁰ is not accompanied by augmented inhibitory potency against TK-2 [IC₅₀ ≈ 3 μM]; (iii) the evaluation of the effect of substituents attached at the distal site of the compounds indicated that aromatic substituents such as diphenylmethyl, biphenyl, and dibenzyl result in potent TK inhibition, although the triphenylmethyl (trityl) moiety still afforded the most pronounced inhibitory values.^{10,12–14} With all this information in hand, we considered that the next generation of compounds should keep the thymine base intact to interact at the substrate binding site as well as an *O*-trityl moiety at the distal site because this substituent has afforded the best inhibitory values so far. On the basis of the conformational flexibility of TK-2 and similar kinases,^{15,16} we decided to tether the thymine base with the distal *O*-trityl through polymethylene spacers of different lengths and to evaluate the

impact of these modifications on TK-2 inhibition. Compounds bearing a less hydrophobic diethyleneglycol-based tether also have been synthesized. Moreover, several substituents have been incorporated at position 4 of one of the phenyl rings of the trityl moiety to determine the role of such substitutions on TK-2 inhibition.

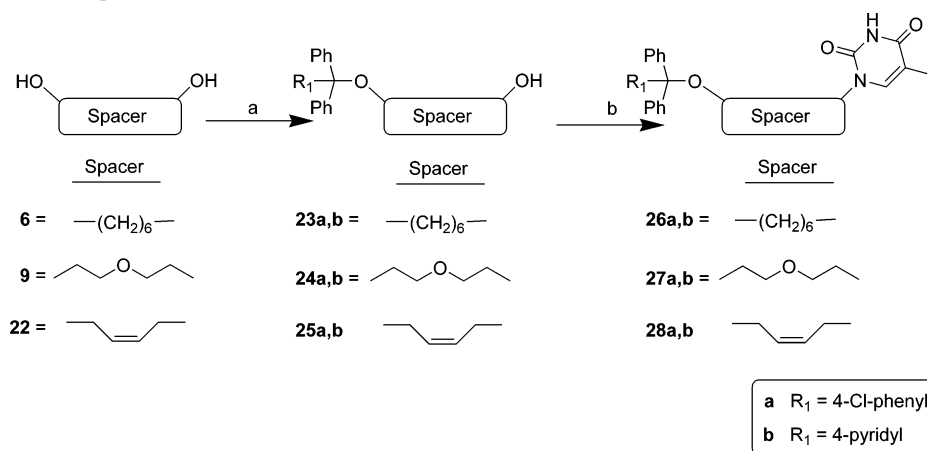
Chemistry

The approach followed to synthesize the tethered molecules in which the thymine base is connected with the distal *O*-trityl through different polymethylene spacers is shown in Scheme 1 and basically consisted of monotritylation on the symmetrical diol followed by introduction of the thymine base under Mitsunobu conditions.¹⁰ There have been different approaches to the selective monoprotection of symmetric diols; one of the most common procedures involves the use of a large excess of the diol relative to the protecting reagent (typically if the diol is inexpensive).¹⁷ Thus, reaction of an excess of the alkanediols (**4–8**; *n* = 3, 5–8) with trityl chloride (used as the limiting reagent) in CH₂Cl₂ and in the presence of Et₃N and DMAP afforded the monotrityl alcohols **10–14** with yields that ranged from 83 to 96%. Reaction of diethylene glycol (**9**) with trityl chloride under similar conditions afforded the *O*-trityl derivative **15** in 50% yield. Condensation of the alcohols **10–15** with *N*³-benzoylthymine¹⁸ in the presence of PS-triphenylphosphine and diisopropyl azodicarboxylate (DIAD) in dry THF afforded the coupling products that were immediately debenzoylated by treatment with 1 M NaOH in a dioxane/H₂O (1:1) solution. In every case, the only condensation product detected was the alkylated compound at *N*-1 of the thymine ring. Yields of the targeted compounds (**16–21**) range from 60 to 74%. When compounds **16–21** were evaluated against TK-2-catalyzed dThd phosphorylation (see Biological Results), it was found that the length of the tether had a major impact on enzyme inhibition; the best results were obtained with the six-methylene compound **18**, which was even more active than the prototype (*Z*)-2-butenyl derivative **1**. The diethylglycol derivative **21** was slightly less active, but the less lipophilic character of this molecule (see cLogP values in Supporting Information) prompted us to consider it as a good candidate for further structural exploration.

Therefore, we next focused on introduction of modifications on the trityl moiety. These modifications included replacement of one of the phenyl rings of the trityl by either a 4-chlorophenyl or a 4-pyridyl ring as shown in series **26–28a,b** (Scheme 2). The synthetic approach was very similar to that described in Scheme 1 with the only exception that the corresponding trityl chlorides had to be synthesized. (4-Chlorophenyl)diphenyl-

Scheme 1. Synthesis of Compounds **16–21**^a

^a (a) TrCl, DMAP, Et₃N, CH₂Cl₂; (b) 1. *N*³-BzT, PS-Ph₃P, DIAD, THF; 2. Dioxane/1 M NaOH (1:1).

Scheme 2. Synthesis of Compounds 26–28a,b^a

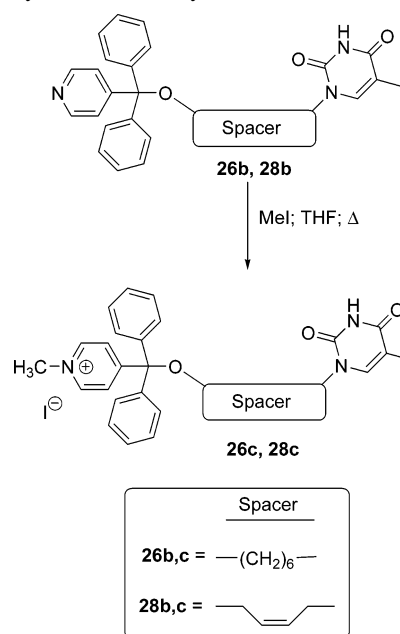
^a (a) 4-Cl-trityl chloride (a series) or 4-pyridyldiphenylmethyl chloride (b series), DMAP, Et₃N, CH₂CH₂; (b) 1. N³-BzT, PS-Ph₃P, DIAD, THF; 2. Dioxane/1 M NaOH (1:1).

carbinol was prepared by reaction of the 4-chlorobenzophenone with phenylmagnesium bromide, following described procedures,¹⁹ and was further transformed into the desired chloride by reaction with acetyl chloride.¹⁹ Reaction of this chloride with alcohols **6**, **9**, and **22**, in CH₂Cl₂ and in the presence of Et₃N and DMAP, afforded the monosubstituted compounds (**23a**, **24a**, and **25a**) in 63–86% yield (Scheme 2). Incorporation of the thymine base in a similar way as described in Scheme 1, followed by treatment with 1 N NaOH in dioxane, afforded the *N*-1-substituted thymine derivatives **26a**, **27a**, and **28a** in 55, 56, and 70% yield, respectively.

On the other hand, the commercially available diphenyl-4-pyridylmethanol was transformed into the corresponding chloride²⁰ and reacted with **6**, **9**, and **22** to afford the monosubstituted alcohols **23b**, **24b**, and **25b** in 84, 58 and 34% yield, respectively (Scheme 2). Mitsunobu-type condensation with *N*³-benzoylthymine,¹⁸ followed by basic deprotection, afforded the desired compounds **26b**, **27b**, and **28b** in 75, 62, and 56% yield, respectively. Compounds **26b** and **28b** were further transformed into the corresponding *N*-methylpyridinium salts by reaction with methyl iodide in THF (Scheme 3) to afford compounds **26c** and **28c** in 73 and 47% yield, respectively.

Another modification that was considered of interest was the introduction of a carboxamide moiety at position 4 of one of the phenyl rings of the trityl moiety. It has been reported that 4-carboxy derivatives of trityls are 2–5 times more stable to acidic treatment than the corresponding non-substituted analogues.²¹ Moreover, the introduction of the carboxamide moiety at the trityl is suitable to further functionalize the compounds through the amide moiety. On the basis of previous reports,^{21–23} prior to transformation of the carbinol to the chloride, the 4-(hydroxydiphenylmethyl)benzoic acid was transformed to the corresponding *N*-succinimidyl benzoate. Once protected at the carboxylic acid, the carbinol was reacted with acetyl chloride to yield *N*-succinimidyl-(4-chlorodiphenylmethyl)benzoate. The reactions between this trityl chloride and the diols **6** and **22** were performed at 0 °C, as reported in similar cases,²¹ to prevent the possible formation of ester bonds between the excess of the diol and the activated *N*-succinimidyl benzoate. In this way, the monotritylated compounds **29** and **30** were obtained in 25 and 44% yield, respectively (Scheme 4). Reaction of the alcohols **29** and **30** with *N*³-benzoylthymine¹⁷ under Mitsunobu-type condensation conditions, afforded the corresponding coupling products. Further treatment with methylamine in MeOH led to the removal of the *N*³-benzoyl group from thymine together with

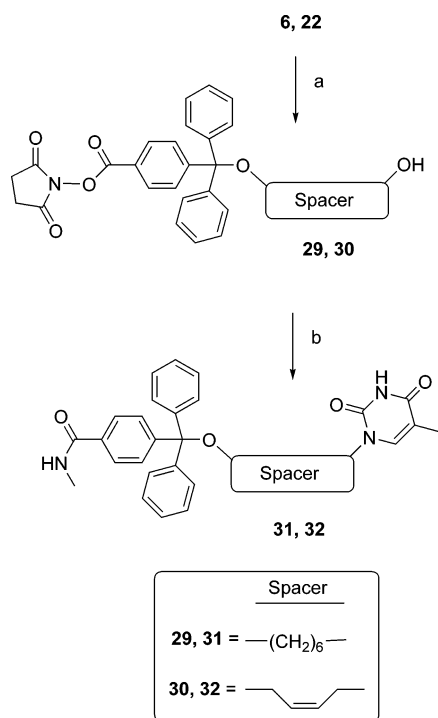
Scheme 3. Synthesis of the Pyridinium Salts 26c and 28c



the transformation of the *N*-succinimidyl benzoate into the corresponding methylbenzamide to afford the targeted compounds **31** and **32** in 33 and 40% yield, respectively.

Biological Results and Discussion

Inhibition of [methyl-³H]dThd Phosphorylation by TK-2, HSV-1 TK, and *Dm*-dNK. Compounds **16–21**, **26–28(a–c)**, **31**, and **32** were tested for their inhibitory effect against phosphorylation of 1 μM thymidine by recombinant TK-2, HSV-1 TK, and *Dm*-dNK. The results are shown in Table 1. The lead compound **1** has also been included in the table for comparative purposes. Evaluation of the *N*¹-thymine-tethered-*O*-trityl derivatives **16–21** clearly showed a strong relationship between the length of the spacer and the inhibitory activity against the tested enzymes. Short ($n = 3$; **16**) or long ($n = 8$; **20**) polymethylene linkers afforded TK-2 inhibition around 45 μM, while intermediate length linkers afforded higher inhibitory values. In particular, a hexamethylene linker ($n = 6$; **18**) gave the highest inhibitory potency with an IC₅₀ of 0.50 μM. Interestingly, replacement of the middle carbon by oxygen in the five-methylene linker (**21** versus **17**) slightly reduced the

Scheme 4. Synthesis of the Carboxamide Derivatives **31** and **32**^a

^a (a) *N*-Succinimidyl-(4-chlorodiphenylmethyl)benzoate, DMAP, Et₃N, CH₂CH₂, 0 °C; (b) 1. N³-BzT, PS-Ph₃P, DIAD, THF; 2. MeNH₂/MeOH, rt.

Table 1. Inhibitory Effect of the Test Compounds on the Phosphorylation of 1 μM [*methyl*-³H]dThd by TK-2, HSV-1 TK, and *Dm*-dNK

comp	IC ₅₀ ^a (μM)		
	TK-2	HSV-1 TK	<i>Dm</i> -dNK
1	1.5 ± 0.2	45 ± 1	3.3 ± 0.9
16	45 ± 2	46 ± 5	21 ± 6
17	2.5 ± 0.4	32 ± 1	15 ± 2
18	0.50 ± 0.01	3.7 ± 0.5	17 ± 10
19	4.7 ± 0.5	≥ 50	32 ± 8
20	45 ± 7	> 500	30 ± 14
21	9.7 ± 0.1	17 ± 4	56 ± 21
26a	1.9 ± 0.7	1.0 ± 0.9	47 ± 1
26b	0.47 ± 0.03	2.0 ± 0.4	2.7 ± 0.2
26c	23 ± 1	41 ± 6	29 ± 1
27a	5.2 ± 1.7	2.7 ± 0.0	45 ± 6
27b	23 ± 0.3	21 ± 0	35 ± 2
28a	2.4 ± 1.2	18 ± 7	5.7 ± 2.4
28b	1.8 ± 0.1	25 ± 2	3.4 ± 0.1
28c	114 ± 71	> 500	144 ± 58
31	0.39 ± 0.03	0.7 ± 0.4	3.5 ± 0.1
32	1.9 ± 0.2	42 ± 4	1.6 ± 0.7

^a 50% inhibitory concentration required to inhibit enzyme-catalyzed dThd phosphorylation by 50%.

inhibitory potency against TK-2. It is worth mentioning that the length of the linker has a major impact on inhibition of HSV-1 TK. Whereas compound **18** (*n* = 6) gave also the best inhibitory value against HSV-1 TK (IC₅₀ = 3.7 μM), longer linkers resulted in annihilation of activity (i.e., compound **20**). In contrast, the length of the linker has a much less important impact on inhibition of *Dm*-dNK.

Attention was next paid to the role of substituents in one of the phenyl rings of the triphenyl moiety, and this effect was studied in molecules with three different spacers: a hexamethylene, a (2-ethoxy)ethyl, and a (*Z*)-2-butenyl, the latter being present in our lead compound **1**. These series of compounds were very helpful to confirm that the linker impinges greatly

on potency and selectivity against the target enzymes. In every case, the compounds carrying a hexamethylene spacer (**26a–b**, **31**) afforded the best inhibitory values against TK-2, followed by the (*Z*)-2-butenyl derivatives (**28a,b**, **32**), while the (2-ethoxy)ethyl derivatives (**27a,b**) were less active, as already seen in the unsubstituted trityl series. It is also interesting to note that the (*Z*)-2-butenyl derivatives (**28a,b**, **32**) show a higher discrimination between TK-2 and HSV-1 TK than do the compounds with the other two spacers. The only modification that clearly has a deleterious effect on the inhibitory potency against the three enzymes is the introduction of the pyridinium salt in the trityl moiety (compare compounds **26b** to **26c**, and **28b** to **28c**). To explain the much weaker potency of **26c** and **28c** compared to the parent pyridine derivatives **26b** and **28b**, steric hindrance could not be involved on the basis of the inhibitory potency of the 4-Cl- or 4-carboxamide substituted derivatives. However, it might be considered that the ionic nature of the salts **26c** and **28c** could be responsible for unfavorable interactions with the enzyme. It is indeed well possible that the trityl moiety of the TK-2 inhibitors interacts with a highly lipophilic pocket in the enzyme that does not allow charged (polar) entities. Alternatively, the desolvation of these charged molecules required to efficiently interact with the enzyme, may involve an important entropic penalty that compromises the interaction with the target enzyme.

Detailed kinetic analyses were then performed with **26b**, one of the most potent inhibitors against TK-2 described. When tested against dThd as a variable substrate (in the presence of saturating concentrations of ATP), **26b** showed a purely competitive inhibition of TK-2, with a *K_i* value of 0.29 μM, resulting in a *K_i/K_m* ratio of 0.32. This means that the affinity of the TK-2 inhibitor for the enzyme is at least as good as, if not higher than, that of the natural substrate dThd. The more potent inhibition of TK-2 by **26b** compared to that exerted by the prototype compound **1** is also reflected in a lower *K_i* value (0.29 versus 0.50 μM). When the 4-pyridyl derivative **26b** was tested against variable concentrations of ATP, which is the cosubstrate of the TK-2-catalyzed reaction, it behaved as an uncompetitive inhibitor of TK-2, with a *K_i* value of 10 μM. Since the *K_m* value for ATP is 19 μM, the *K_i/K_m* ratio is 0.54. The profile showing competitive and uncompetitive inhibition against thymidine and ATP, respectively, is similar to that previously observed with our prototype compound **1**.¹² The uncompetitive inhibition against ATP indicates that compounds such as **26b** and **1** would only bind to TK-2 after ATP is bound as a cosubstrate. In the light of the competitive inhibition against dThd, it can be surmised that compounds **1** and **26b** bind at the dThd-binding site of the enzyme, but they can only do so once ATP is already bound to the enzyme. This suggests that ATP binding may promote a conformational change at the substrate-binding site that allows entry and stabilization of the inhibitors.

It may be worth mentioning that the most active TK-2 inhibitors revealed in this study are not inhibitory to cytosolic TK-1 (data not shown). These findings suggest the lack of an appropriate binding pocket in TK-1, and thus stress the selectivity of the described TK-2 inhibitors in this study.

Molecular Modeling. Since there are no crystal structures currently available for TK-2, we endeavored to build a reliable molecular model of this enzyme that could be used to shed light on the experimentally obtained data. The mGenTHREADER profile-based fold recognition method²⁴ identified several putative structural neighbors of TK-2, most notably the human enzymes deoxycytidine kinase (dCK) and deoxyguanosine kinase (dGK), and the fruitfly, *D. melanogaster* deoxyribo-

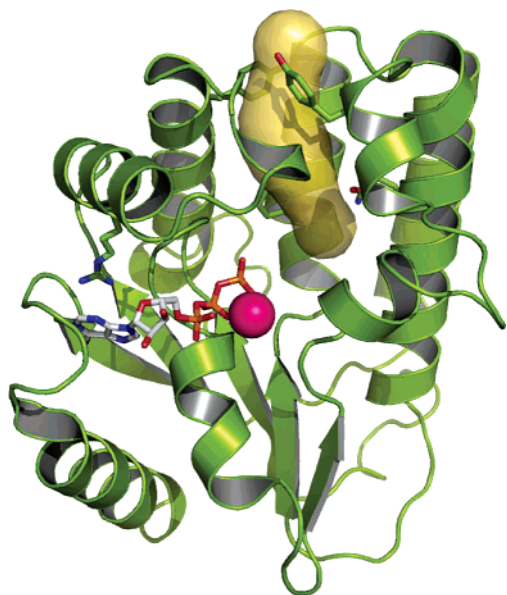


Figure 1. Schematic ribbon representation of modeled TK-2 following deformation along the first non-translational, non-rotational normal mode.³⁷ The “cryptic” tunnel exposed at the interhelical region that is proposed to be the binding site for the inhibitors’ linkers is depicted as a semitransparent yellow surface and is seen to connect the thymidine-binding site to the bulk solvent. Bound ATP-Mg²⁺ is shown for reference only as these ligands were not explicitly taken into consideration in the normal modes calculation. For greater clarity, the side chains of Arg159 (stacking over the adenine ring of ATP), Gln77, Tyr66, and Tyr175 are displayed as sticks. Note the varying width of this tunnel which is narrowest at the plane delineated by these Tyr residues.

nucleotide kinase (*Dm*-dNK), with percentages of sequence identity of 29.3, 17.7, and 47.7%, respectively, over about 220 amino acids (Supporting Information, Figure S1). All of these enzymes belong to the same homologous superfamily of P-loop-containing nucleotide triphosphate hydrolases characterized by a three-layer ($\alpha\beta\alpha$) sandwich architecture and a Rossmann fold.

Examination of the normal modes for these enzymes revealed interesting motions that coupled closure of the P-loop in the ATP-binding site with the packing of α -helices 3, 4, 6, and 7 (data not shown). We thought that these conformational changes could be of relevance for our studies because the kinetic analysis data indicated that the hexamethylene derivative **26b** binds at the dThd-binding site of TK-2 only when ATP is already bound, and also because we had previously proposed a model for binding of **1** in which the thymine base is lodged in the dThd-binding site and the triphenylmethoxy substituent is placed in an interhelical hydrophobic region.¹⁴ In fact, the simulated motions in TK-2 (Supporting Information, Figure S2) and further exploration with CASTp²⁵ and CAVER²⁶ servers support the view that a rather hydrophobic tunnel connecting the thymidine-binding pocket with the solvent can be formed at the interface between α -helices 3, 5, and 8, particularly when alternative locations for the side chains of Tyr66 and Tyr175 are found (Figure 1). Furthermore, when this region was explored with the automated docking program AutoDock, the best-scoring solution for **1**, **18**, and **26b** indeed placed the thymine moiety inside the dThd-binding cavity with the planar heteroaromatic ring sandwiched between the phenyl ring of Phe110 on one side and the side chains of both Trp53 and Val80 on the other side, whereas O4 and N3 establish good hydrogen bonds with the carboxamide group of Gln77 (Figure 2). The spacer attached to the thymine exits this cavity at right angles from the ATP-

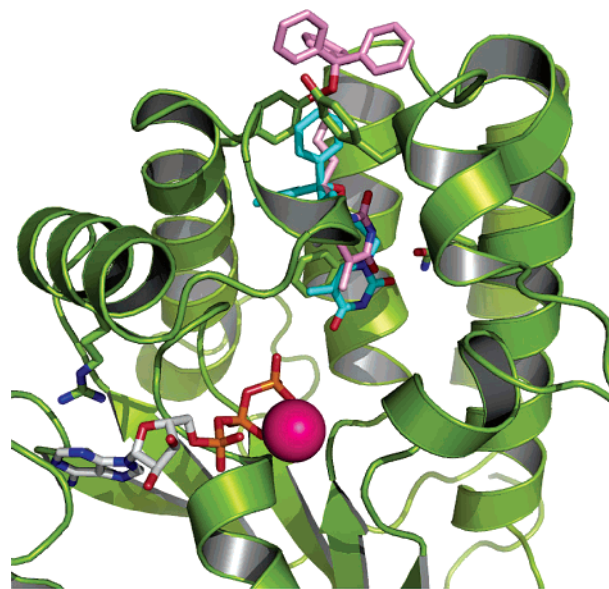


Figure 2. AutoDock best-scoring poses for inhibitors **1** (C atoms in cyan) and **18** (C atoms in pink) docked into the proposed binding site of TK-2, which is displayed as a ribbon in olive green. Note the almost perpendicular disposition of these inhibitors relative to ATP, and the interactions of the trityl group with the Tyr residues just below or above the plane delineated by these aromatic residues.

binding site and traverses a tunnel made up of the hydrophobic side chains of Ile26, Leu62, Met65, Tyr66, Leu76, Leu114, Ile171, and Tyr175 (Figure 2). Depending on the length of the spacer, the distal triaryl moiety of **1**, **18**, and **26b** will be positioned in a plane below ($n = 4$) or above ($n = 6$) the aromatic rings of Tyr66 and Tyr175, thus allowing these rings to establish favorable stacking and edge-to-face interactions. If the spacer is shorter, these interactions cannot take place, and the inhibitor is strained in the interhelical region. This results in the decreased potency observed in going from **18** to **17** and **16**. Increasing the length of the spacer results in a worsening of these interactions and increased exposure to the solvent, both of which also have a detrimental effect on the inhibitory activity, as in going from **18** to **19** and **20**. The model also accounts for the experimental findings that the introduction of substituents such as a Cl (**26a**, **27a**, **28a**) or a methylcarboxamide in the para position of one of the phenyl rings of the triphenylmethoxy moiety does not affect the potency because this group is facing the solvent and therefore does not contribute to the affinity. On the other hand, the loss of potency in **26c** and **28c** relative to **26b** and **28b** can be attributed to the unfavorable effect on the electrostatic edge-to-face interaction of replacing the pyridine ring with a methylpyridinium cation. With respect to the loss in activity brought about by the replacement of a methylene unit (**26**) by an ether oxygen (**27**), the model indicates that the region lodging the spacer is found in the hydrophobic environment provided by Ile26 and Ile179, hence the deleterious effect of having the polar oxygen in this position. The fact that the longer alkyl spacers found in **19** and **20** lead to a highly significant loss of activity against HSV-1 TK can also find an explanation from the multiple sequence and structural alignment: this enzyme shows indeed a longer $\alpha 3$ helix that places the N-terminus of helix $\alpha 4$ as a lid over the putative binding site, thus hindering lodging of the trityl group.

Evaluation of Compounds 18 and 26b in the Intact OST-TK⁻/HSV-1 TK⁺ cells. The low levels of TK-2 compared to the abundant cytosolic TK-1, together with its mitochondrial localization, have been proposed as two major reasons that

Table 2. Effect of Compounds **18** and **26b** on the Cytostatic Activity of Ara-T and GCV in OST-TK⁻/HSV-1 TK⁺ Cell Lines

inhibitor (conc)	IC ₅₀ ^a (μM)	
	Ara-T	GCV
none	0.0062 ± 0.0015	0.0019 ± 0.000
18 (10 μM)	0.15 ± 0.01	0.041 ± 0.013
(5 μM)	0.10 ± 0.02	0.033 ± 0.000
(2.5 μM)	0.055 ± 0.002	0.018 ± 0.002
26b (10 μM)	0.37 ± 0.00	0.11 ± 0.01
(5 μM)	0.24 ± 0.03	0.081 ± 0.013
(2.5 μM)	0.12 ± 0.02	0.050 ± 0.005

^a 50% inhibitory concentration required to inhibit cell proliferation by 50%. Data are the mean (±SD) of at least two to three independent experiments.

explain why direct evaluation of TK-2 inhibitors in cell culture is difficult. The expression of TK-2 in the cytosol of tumor cell lines by a TK-2 gene construct has been unsuccessful so far. However, based on the existing similarities between TK-2 and HSV-1 TK, and since some of the TK-2 inhibitors described herein also significantly inhibit HSV-1 TK, the effect of two of the most potent inhibitors (**18** and **26b**) was evaluated in intact HSV-1 TK-expressing OST-TK⁻/HSV-1 TK⁺ cell cultures in combination with compounds that are good substrates for HSV-1 TK, including the pyrimidine nucleoside 1-(β-D-arabinofuranosyl)thymine (Ara-T) and the purine derivative ganciclovir (GCV) (Table 2). The OST-TK⁻/HSV-1 TK⁺ cells represent human osteosarcoma cells that are deficient in cytosolic TK-1 but express HSV-1 TK in the cytosol.²⁷ It is well-established that when the substrates Ara-T and GCV are added to OST-TK⁻/HSV-1 TK⁺ cell cultures, a marked cytotoxicity is observed with IC₅₀ values in the low nanomolar range (0.0062–0.0019 μM). Addition of the HSV-1 TK inhibitor **18** at a concentration of 10 μM to these cultures markedly reduced the cytotoxic effect of Ara-T and GCV by 24- and 22-fold, respectively. This effect is clearly dose-dependent since addition of lower concentrations of the inhibitor **18** (5 and 2.5 μM) has, as expected, a less pronounced effect on the IC₅₀ values of Ara-T and GCV. Interestingly, addition of compound **26b** to the cell cultures at a concentration of 10 μM has a more pronounced effect on the cytotoxicities of Ara-T and GCV, which were reduced by 60- and 58-fold, respectively, compared to the untreated cell cultures. This “detoxifying” effect of compound **26b** is also dose-dependent, as shown in Table 2. The more pronounced effect of compound **26b** compared to that of **18** in cell culture could not be ascribed to significant differences in the inhibition of the target enzyme HSV-1 TK as shown in the enzymatic assay (IC₅₀ values against HSV-1 TK of 2.0 and 3.7 μM, respectively). Therefore, it could be suggested that the presence of the pyridine ring in the triaryl substituent in **26b** slightly reduces the LogP value of these lipophilic molecules compared to the triphenyl derivative **18**, resulting in a better behavior (solubility and/or uptake) in the cells. Calculated LogP values of these and other compounds in this paper are included as Supporting information. Replacement of a phenyl by a pyridyl is a well-established approach in bioisosterism, and recent examples can be found in the literature.²⁸

The dose-dependent reversal of the AraT- and GCV-related cellular toxicity by the TK-2 (and HSV-1 TK) inhibitors thus strongly suggest that these compounds efficiently penetrate into the intact tumor cells and are able to reach their target enzyme in the intracellular environment when present in the cytosol. Experiments are underway to reveal whether the test compounds are also able to cross the mitochondrial double membrane in the intact cells.

Conclusions

On the basis of our previous results on the inhibitory activity of **1** against TK-2-catalyzed dThd phosphorylation, a variety of novel N¹-substituted thymine derivatives were synthesized and investigated as inhibitors of TK-2 and related enzymes (*Dm*-dNK and HSV-1 TK). The length of the spacer connecting the thymine base and the distal triphenylmethoxy moiety was also varied, having an important impact on inhibitory activity. Moreover, modifications were performed on one of the phenyl rings of the trityl group including incorporation of a 4-Cl or 4-CONHCH₃ substituent or replacement of one of the phenyl rings by 4-pyridyl or a 4-pyridinium salt. Thus, by modifying the linker and the substitution on the trityl moiety, a 4-fold gain in potency against TK-2-catalyzed dThd phosphorylation was achieved relative to our previous lead compound **1**.

Compound **26b** has been shown to be a competitive inhibitor against TK-2 when dThd is used as a variable substrate ($K_i = 0.29 \mu\text{M}$) and an uncompetitive inhibitor when tested against variable concentrations of ATP. The molecular model we have built accounts for this fact as the thymine ring of the inhibitors is proposed to occupy the thymidine-binding site in a standard orientation, whereas the spacer would extend toward the surface through a hydrophobic channel that is not present in the resting state but whose existence is made apparent when an elastic network model of the enzyme is considered. This finding strongly suggests that the methodology employed in this work could be useful for other targets in which “cryptic” binding sites are exposed following a local rearrangement of the protein backbone.²⁹

Among the very few molecules reported in the literature that inhibit TK-2-catalyzed dThd phosphorylation, compounds **18**, **26b**, and **31** represent three of the most potent inhibitors described so far. Moreover, compound **26b** has been recently shown to be a useful tool to evaluate the specific TK-2 activity in human fibroblasts and has been instrumental to set up a new assay to measure TK-2 expression in cultured cells and for the determination of TK-2 activity in patient samples.³⁰ Finally, a TK-2 inhibitor may be useful to investigate the role of TK-2 in mitochondrial homeostasis in general and in the regulation of the mitochondrial deoxynucleotide pools in particular.

Experimental Section

Chemical Procedures. Melting points were obtained on a Reichert-Jung Kofler apparatus and are uncorrected. Microanalyses were obtained with a Heraeus CHN-O-RAPID instrument. Electrospray mass spectra were measured on a quadrupole mass spectrometer equipped with an electrospray source (Hewlett-Packard, LC/MS HP 1100). ¹H and ¹³C NMR spectra were recorded on a Varian Gemini operating at 200 MHz (¹H) and 50 MHz (¹³C), respectively, on a Varian INNOVA 300 operating at 299 MHz (¹H) and 75 MHz (¹³C), respectively, and a Varian INNOVA-400 operating at 399 MHz (¹H) and 99 MHz (¹³C), respectively.

Analytical TLC was performed on silica gel 60 F₂₅₄ (Merck) precoated plates (0.2 mm). Spots were detected under UV light (254 nm) and/or by charring with phosphomolibdic acid. Separations on silica gel were performed by preparative centrifugal circular thin layer chromatography (CCTLC) on a ChromatotronR (Kiesegel 60 PF₂₅₄ gipshaltig (Merck)), layer thickness (1 or 2 mm), flow rate (4 or 8 mL/min, respectively). Flash column chromatography was performed with silica gel 60 (230–400 mesh) (Merck).

Polystyrene-triphenylphosphine (PS-Ph₃P) was purchased from Fluka. DIAD was purchased from Aldrich.

All experiments involving water-sensitive compounds were conducted under scrupulously dry conditions. Triethylamine and acetonitrile were dried by refluxing over calcium hydride. Tetrahy-

dofuran was dried by refluxing over sodium/benzophenone. Anhydrous *N,N'*-dimethylformamide was purchased from Aldrich.

General Procedure for Monotrylation of Diols. To a stirred solution of the corresponding diol (10 mmol) in dry CH_2Cl_2 (4 mL) at 0 °C, Et_3N (0.15 mL, 1.1 mmol), DMAP (5 mg, 0.04 mmol) and trityl chloride (278 mg, 1.0 mmol) were added. The mixture was stirred at rt for 24 h. Then, it was diluted with CH_2Cl_2 (20 mL) and water (10 mL). The organic phase was washed with water (10 mL), and brine (10 mL). (The excess diol was removed in these washing steps.) The organic layer was dried on anhydrous Na_2SO_4 , filtered, and evaporated. The residue was purified by flash column chromatography.

General Procedure for the Mitsunobu Condensation of Alcohols with *N*³-Benzoylthymine. To a suspension containing the corresponding alcohol (**10–15**, **23–25a,b**) (0.5 mmol), $\text{PS-Ph}_3\text{P}$ (3 mmol/g, 416 mg, 1.25 mmol), and *N*³-benzoylthymine (230 mg, 1.0 mmol) in dry THF (5 mL), a solution of DIAD (0.19 mL, 1.0 mmol) in dry THF (2 mL) was slowly added. The mixture was stirred at rt overnight. The reaction was filtered, the residue was washed with THF (2 × 5 mL), and the combined filtrates were evaporated to dryness. The residue was dissolved in a dioxane/NaOH 1M (1:1) mixture (9 mL) and stirred overnight. Then, EtOAc (10 mL) and brine (5 mL) were added. The aqueous phase was further extracted with EtOAc (3 × 10 mL). The combined organic extracts were dried on anhydrous Na_2SO_4 , filtered, and evaporated. The residue was purified in the chromatotron CCTLC (hexane-EtOAc, 1:1) to yield the target compounds.

Data for compounds **10–32** are provided as Supporting Information.

TK Assay Using [*methyl*-³H]dThd as the Substrate. The activity of recombinant TK-2, HSV-1 TK, and *Dm*-dNK, and the 50% inhibitory concentration of test compounds were assayed in a 50- μL reaction mixture containing 50 mM Tris/HCl, pH 8.0, 2.5 mM MgCl_2 , 10 mM dithiothreitol, 0.5 mM CHAPS, 3 mg/mL bovine serum albumin, 2.5 mM ATP, and 1 μM [*methyl*-³H]dThd and enzyme. The samples were incubated at 37 °C for 30 min in the presence or absence of different concentrations (5-fold dilutions) of the test compounds. The reaction proceeded linearly during this time period. After the incubation period, aliquots of 45 μL of the reaction mixtures were spotted on Whatman DE-81 filter paper disks. The filters were washed three times for 5 min each in 1 mM ammonium formate, once for 1 min in water, and once for 5 min in ethanol. The radioactivity was determined by scintillation counting.

The K_m values (for dThd and ATP) and the K_i values for the inhibitor **26b** using varying concentrations of dThd (ranging between 0.4 and 5 μM) at saturating concentrations of ATP (2.5 mM) or using varying concentrations of ATP (ranging between 5 and 250 μM) at saturating concentrations of dThd (20 μM) were determined and derived from Lineweaver–Burk plots.

Computational Methods. Comparative Modeling of Human TK-2. The amino acid sequence of human mitochondrial thymidine kinase (KITM_HUMAN) was retrieved from Swiss-Prot (<http://us.expasy.org/sprot/>). The mGenTHREADER profile-based fold recognition method²⁴ was used to predict the secondary structure of human TK-2 and to identify putative structural neighbors, which were found to be in agreement with the FSSP/Dali classification.³¹ The multiple structural alignment of the eight proteins with the highest Dali scores (human deoxycytidine kinase [1p60], human deoxyguanosine kinase [1jag], *Drosophila melanogaster* deoxyribonucleotide kinase [1oe0], herpes simplex virus 1 thymidine kinase [1p7e], equine herpes virus thymidine kinase [1p6x], yeast thymidylate kinase [3tmk], *Escherichia coli* thymidylate kinase [4tmk], and human thymidylate kinase [1e2f]) was performed using the Mammoth server³² (Supporting Information, Figure S1). Because of the greater sequence identity, *Dm*-dNK was used as the template for homology modeling of TK-2 except for the predicted C-terminal α -helix (α_9) whose counterpart is missing in this crystal structure. This α -helix was taken from the netrin-like domain of human procollagen C-proteinase enhancer (PCOLCE) protein (PDB code 1uap)³³ and superimposed on the equivalent helix found in human

dGK (PDB code 1jag) while retaining the connecting loop (204–210) conformation found in dCK (PDB code 1p60). The loops comprising amino acids 43–44 and 192–193 were modeled by satisfaction of spatial restraints using the ModLoop server.³⁴ Amino acid replacement and rotamer selection were performed using the built-in facility available in PyMOL.³⁵ ATP- Mg^{2+} was incorporated into the structure by adding the gamma phosphate to the ADP- Mg^{2+} already present in the structure of human dCK so as to reproduce the conformation of the nonhydrolyzable analogue of ATP found in human thymidylate kinase (PDB code 1e2q).

Normal-Mode Analyses and Cavity Calculations. To probe the flexibility of this family of enzymes, an elastic network model was used in which all non-hydrogen protein atoms (within a cutoff of 10 Å) were modeled as point masses and C α atoms were connected by springs representing the interatomic force fields.³⁶ Each protein was then analyzed as a large set of coupled harmonic oscillators using the NOMAD-REF server.³⁷ The conformational changes most likely involved in ATP and inhibitor binding were deduced by calculating the 10 lowest-frequency normal modes, which are those with the highest amplitudes and those most often related to large-scale structural rearrangements in proteins. Each mode was explored in its two opposite directions, thus resulting in two structures (“open” and “closed”) different from the initial one within an rmsd value of 2 Å. The areas and volumes of pockets located on the protein surface and voids buried in the protein interior were calculated analytically by means of the CASTp server,²⁵ whereas the CAVER server²⁶ was employed to delineate the shape of the tunnel connecting the dThd-binding site with the bulk solvent.

Docking of Representative Inhibitors. Compounds **1**, **18**, and **26b** were used as ligands for the automated docking experiments. A variety of more “open” TK-2 conformations was selected from the normal modes calculations, and alternative positions for the side chains of Tyr66, Gln77 and Tyr175 were found using the built-in rotamer library implemented in PyMOL. The magnesium ion was assigned a charge of +2, and AMBER-compatible RESP point charges were used for the inhibitors and ATP⁴⁻, as reported previously.¹⁴ The Lamarckian genetic algorithm³⁸ implemented in AutoDock 3.0.5³⁹ was used to generate docked conformations of each inhibitor within the putative binding cavity by randomly changing the overall orientation of the molecule as well as the torsion angles of the different spacers. Default settings were used except for number of runs, population size, and maximum number of energy evaluations, which were fixed at 100, 100, and 250 000, respectively. Rapid intra- and intermolecular energy evaluation of each configuration was achieved by having the receptor’s atomic affinity potentials for aliphatic and aromatic carbon, oxygen, nitrogen, and hydrogen atoms precalculated in a three-dimensional grid with a spacing of 0.375 Å. A distance-dependent dielectric function was used in the computation of electrostatic interactions.

Acknowledgment. A.I.H. and O.F. thank the Spanish Ministerio de Educación y Ciencia for a predoctoral fellowship. This work has been supported by grants from the Spanish MEC (SAF2003-07219-C02 and SAF 2000-0153-C02) (to M.J.C, M.J.P.P., and F.G.), the EU (QLRT-2001-01004) (to M.J.C, M.J.P.P., A.K and J.B.), and the National Foundation for Cancer Research (to F.G.). We thank Mrs. Lizette van Berckelaer for excellent technical assistance.

Supporting Information Available: Synthesis and data for compounds **10–15** and **16–32**. Elemental analysis of compounds **16–21**, **26–28a–c**, **31**, and **32**. Calculated LogP values for compounds **1**, **18**, **21**, **26b**, **27b**, and **28b**. Multiple sequence alignment based on structural superimposition and profile–profile comparison of human mitochondrial TK-2 and related kinases used in the modeling work. This material is available free of charge via the Internet at <http://pubs.acs.org>.

References

- Arner, E. S. J.; Eriksson, S. Mammalian deoxyribonucleoside kinases. *Pharmacol. Ther.* **1995**, *67*, 155–186.

- (2) Eriksson, S.; Munch-Petersen, B.; Johansson, K.; Eklund, H. Structure and function of cellular deoxyribonucleoside kinases. *Cell Mol. Life Sci.* **2002**, *59*, 1327–1346.
- (3) Van Rompay, A. R.; Johansson, M.; Karlsson, A. Substrate specificity and phosphorylation of antiviral and anticancer nucleoside analogues by human deoxyribonucleoside kinases and ribonucleoside kinases. *Pharmacol. Ther.* **2003**, *100*, 119–139.
- (4) Saada, A.; Shaag, A.; Mandel, H.; Nevo, Y.; Eriksson, S.; Elpeleg, O. Mutant mitochondrial thymidine kinase in mitochondrial DNA depletion myopathy. *Nat. Genet.* **2001**, *29*, 342–344.
- (5) Saada, A. Deoxyribonucleotides and disorders of mitochondrial DNA integrity. *DNA Cell Biol.* **2004**, *23*, 797–806.
- (6) Lewis, W.; Dalakas, M. C. Mitochondrial toxicity of antiviral drugs. *Nat. Med.* **1995**, *1*, 417–422.
- (7) Lewis, W.; Day, B. J.; Copeland, W. C. Mitochondrial toxicity of NRTI antiviral drugs: An integrated cellular perspective. *Nat. Rev. Drug Discovery* **2003**, *2*, 812–822.
- (8) Johansson, K.; Ramaswamy, S.; Ljungcrantz, C.; Knecht, W.; Piskur, J.; Munch-Petersen, B.; Eriksson, S.; Eklund, H. Structural basis for substrate specificities of cellular deoxyribonucleoside kinases. *Nat. Struct. Biol.* **2001**, *8*, 616–620.
- (9) Mikkelsen, N. E.; Johansson, K.; Karlsson, A.; Knecht, W.; Andersen, G.; Piskur, J.; Munch-Petersen, B.; Eklund, H. Structural basis for feedback inhibition of the deoxyribonucleoside salvage pathway: Studies of the *Drosophila* deoxyribonucleoside kinase. *Biochemistry* **2003**, *42*, 5706–5712.
- (10) Hernández, A. I.; Balzarini, J.; Karlsson, A.; Camarasa, M. J.; Pérez-Pérez, M. J. Acyclic nucleoside analogues as novel inhibitors of human mitochondrial thymidine kinase. *J. Med. Chem.* **2002**, *45*, 4254–4263.
- (11) Pérez-Pérez, M. J.; Hernández, A. I.; Priego, E. M.; Rodríguez-Barrios, F.; Gago, F.; Camarasa, M. J.; Balzarini, J. Mitochondrial thymidine kinase inhibitors. *Curr. Top. Med. Chem.* **2005**, *5*, 1205–1219.
- (12) Balzarini, J.; Hernández, A. I.; Roche, P.; Esnouf, R.; Karlsson, A.; Camarasa, M. J.; Pérez-Pérez, M. J. Non-nucleoside inhibitors of mitochondrial thymidine kinase (TK-2) differentially inhibit the closely related herpes simplex virus type 1 TK and *Drosophila melanogaster* multifunctional deoxynucleoside kinase. *Mol. Pharmacol.* **2003**, *63*, 263–270.
- (13) Priego, E. M.; Balzarini, J.; Karlsson, A.; Camarasa, M. J.; Pérez-Pérez, M. J. Synthesis and evaluation of thymine-derived carboxamides against mitochondrial thymidine kinase (TK-2) and related enzymes. *Bioorg. Med. Chem.* **2004**, *12*, 5079–5090.
- (14) Hernández, A. I.; Balzarini, J.; Rodríguez-Barrios, F.; San-Félix, A.; Karlsson, A.; Gago, F.; Camarasa, M. J.; Pérez-Pérez, M. J. Improving the selectivity of acyclic nucleoside analogues as inhibitors of human mitochondrial thymidine kinase: Replacement of a triphenylmethoxy moiety with substituted amines and carboxamides. *Bioorg. Med. Chem. Lett.* **2003**, *13*, 3027–3030.
- (15) Bissantz, C.; Folkers, G.; Rognan, D. Protein-based virtual screening of chemical databases. 1. Evaluation of different docking/scoring combinations. *J. Med. Chem.* **2000**, *43*, 4759–4767.
- (16) Barroso, J.; Carvalho, R.; Flatmark, T. Kinetic analysis and ligand-induced conformational changes in dimeric and tetrameric forms of human thymidine kinase 2. *Biochemistry* **2005**, *44*, 4886–4996.
- (17) Komiotis, D.; Currie, B. L.; LeBreton, G. C.; Venton, D. L. Preparation of monotrylated symmetric 1,n-diols. *Synth. Commun.* **1993**, *23*, 531–534.
- (18) Cruikshank, K. A.; Jiricny, J.; Reese, C. B. The benzylation of uracil and thymine. *Tetrahedron Lett.* **1984**, *25*, 681–684.
- (19) Gibbs, L. W.; Wedegaertner, D. K. A kinetic-study of the rearrangement of triarylacetonitrile oxides. *J. Org. Chem.* **1991**, *56*, 7320–7322.
- (20) Coyle, S.; Hallett, A.; Munns, M. S.; Young, G. T. Amino-acids and peptides 45. The protection of the thiol function of cysteine and the imidazole-N of histidine by the diphenyl-4-pyridylmethyl group. *J. Chem. Soc. Perkin Trans. 1* **1981**, 522–528.
- (21) Shchepinov, M. S.; Chalk, R.; Southern, E. M. Trityl tags for encoding in combinatorial synthesis. *Tetrahedron* **2000**, *56*, 2713–2724.
- (22) Gildea, B. D.; Coull, J. M.; Köster, H. A versatile acid-labile linker for modification of synthetic biomolecules. *Tetrahedron Lett.* **1990**, *31*, 7095–7098.
- (23) Coull, J. M.; Gildea, B. D.; Köster, H. U.S. Patent 5,410,068, 1995.
- (24) McGuffin, L. J.; Smith, R. T.; Bryson, K.; Sorensen, S. A. J., D. T. High throughput profile-profile based fold recognition for the entire Human proteome. *BMC Bioinformatics* **2006**, *7*, 288.
- (25) Dundas, J.; Ouyang, Z.; Tseng, J.; Binkowski, A.; Turpaz, Y.; Liang, J. CASTp: computed atlas of surface topography of proteins with structural and topographical mapping of functionally annotated residues. *Nucleic Acid Res.* **2006**, *34* (Web Server issue): W116–118. URL: <http://cast.engr.uic.edu>.
- (26) Petrek, M.; Otyepka, M.; Banas, P.; Kosinova, P.; Koca, J.; Damborsky, J. CAVER: a new tool to explore routes from protein clefts, pockets and cavities. *BMC Bioinformatics* **2006**, *7*, 316. URL: <http://loschmidt.chemi.muni.cz/caver>.
- (27) Degève, B.; Johansson, M.; De Clercq, E.; Karlsson, A.; Balzarini, J. Differential intracellular compartmentalization of herpetic thymidine kinases (TKs) in TK gene-transfected tumor cells. Molecular characterization of the nuclear localization signal of herpes simplex virus type 1 TK. *J. Virol.* **1998**, *72*, 9535–9543.
- (28) Pastorin, G.; Da Ros, T.; Bolcato, C.; Montopoli, C.; Moro, S.; Cacciari, B.; Baraldi, P. G.; Varani, K.; Borea, P. A.; Spalluto, G. Synthesis and biological studies of a new series of 5-heteroarylcarbamoylaminopyrazolo 4,3-e 1,2,4-triazolo 1,5-c pyrimidine s as human A(3) adenosine receptor antagonists. Influence of the heteroaryl substituent on binding affinity and molecular modeling investigations. *J. Med. Chem.* **2006**, *49*, 1720–1729.
- (29) Teague, S. J. Implications of protein flexibility for drug discovery. *Nat. Rev. Drug Discovery* **2003**, *2*, 527–541.
- (30) Franzolin, E.; Rampazzo, C.; Pérez-Pérez, M. J.; Hernández, A. I.; Balzarini, J.; Bianchi, V. Bromovinyl-deoxyuridine: A selective substrate for mitochondrial thymidine kinase in cell extracts. *Biochem. Biophys. Res. Commun.* **2006**, *344*, 30–36.
- (31) Holm, L.; Sander, C. Dali/FSPP classification of three-dimensional protein folds. *Nucleic Acids Res.* **1997**, *25*, 231–234.
- (32) Lupyan, D.; Leo-Macias, A.; Ortiz, A. R. A new progressive-iterative algorithm for multiple structure alignment. *Bioinformatics* **2005**, *21*, 3255–3263. URL: <http://ub.cbm.uam.es/mammoth/mult/>.
- (33) Liepinsh, E.; Banyai, L.; Pintacuda, G.; Trexler, M.; Patthy, L.; Otting, G. NMR structure of the netrin-like domain (NTR) of human type I procollagen C-proteinase enhancer defines structural consensus of NTR domains and assesses potential proteinase inhibitory activity and ligand binding. *J. Biol. Chem.* **2003**, *278*, 25982–25989.
- (34) Fiser, A.; Sali, A. ModLoop: automated modeling of loops in protein structures. *Bioinformatics* **2003**, *19*, 2500–2501. URL: <http://alto.compbio.ucsf.edu/modloop/modloop.html>.
- (35) DeLano, W. PyMOL version 0.99, DeLano Scientific LLC, South San Francisco, California. URL: <http://pymol.sourceforge.net/>.
- (36) Lindahl, E.; Delarue, M. Refinement of docked protein-ligand and protein-DNA structures using low frequency normal mode amplitude optimization. *Nucleic Acids Res.* **2005**, *33*, 4496–4506.
- (37) Lindahl, E.; Azuara, C.; Koehl, P.; Delarue, M. NOMAD-Ref: visualization, deformation and refinement of macromolecular structures based on all-atom Normal Mode Analysis. *Nucleic Acid Res.* **2006**, *34*, (Web Server issue): W52–56. URL: <http://lorenz.immstr-pasteur.fr/nomad-ref.php>.
- (38) Morris, G. M.; Goodsell, D. S.; Halliday, R. S.; Huey, R.; Hart, W. E.; Belew, R. K.; Olson, A. J. Automated docking using a Lamarckian genetic algorithm and an empirical binding free energy function. *J. Comput. Chem.* **1998**, *19*, 1639–1662.
- (39) <http://www.scripps.edu/pub/olson-web/doc/autodock>.